DMD Fast Forward. Published on September 26, 2018 as DOI: 10.1124/dmd.118.081166
This article has not been copyedited and formatted. The final version may differ from this version.

Title Page

Identification and Quantification of Novel Major Metabolites of the Steroidal Aromatase Inhibitor, Exemestane

Shaman Luo*, Gang Chen*, Cristina I. Truica, Cynthia C. Baird, Zuping Xia, Philip Lazarus

Department of Pharmaceutical Sciences, College of Pharmacy, Washington State University, Spokane, WA (S.L., G.C., Z.X., P.L.)

Department of Medicine, Penn State University College of Medicine, Hershey, PA (C.I.T., C.C.B.)

Alkali Soil Natural Environmental Science Center, Northeast Forestry University, Harbin, Heilongjiang, China (S.L.)

* These authors contributed equally to this work.

Downloaded from dmd.aspetjournals.org at ASPET Journals on April 19, 2024

DMD Fast Forward. Published on September 26, 2018 as DOI: 10.1124/dmd.118.081166
This article has not been copyedited and formatted. The final version may differ from this version.

Running Title Page

Running title: Novel Metabolites of Exemestane

Corresponding author: Philip Lazarus, College of Pharmacy, Washington State University, PBS Building Room 431, P.O. Box 1495, Spokane, WA 99202. E-mail: phil.lazarus@wsu.edu

Text Pages: 27 (excluding Abstract page)

Tables: 2

Figures: 5

References: 53

Abstract Word Count: 231

Introduction Word Count: 530

Discussion Word Count: 1,560

Abbreviations:

AIs, Aromatase inhibitors; AZA, azathioprine; CYP, Cytochrome P450s;17β-DHE, 17β-dihydro-EXE; D_3-17β-DHE, 17β-OH-EXE-d3;6-17β-DHE-cys, 6-methylcysteinylandrosta-1,4-diene-17β-hydroxy-3-one; 17β-DHE-Gluc, 17β-hydroxy-EXE-17-O-β-D-glucuronide; D_3-17β-DHE-Gluc, 17β-OH-EXE-d3-17-O-β-D-glucuronide; ER+, estrogen receptor-positive; EXE, Exemestane; D_3-EXE, EXE-19-d3; 6-EXE-cys, 6-methylcysteinylandrosta-1,4-diene-3,17-dione; GSTs, glutathione-*S*-transferases; γ-GT, glutamyltranspeptidase; HLC, human liver cytosol; LC-MS, liquid chromatography-mass spectrometry; NMR, Nuclear Magnetic Resonance**;**TEM, total quantified EXE metabolites; TLC, thin layer chromatography; UPLC-MS, ultra-pressure liquid chromatography-mass spectrometry.

Downloaded from dmd.aspetjournals.org at ASPET Journals on April 19, 2024

DMD Fast Forward. Published on September 26, 2018 as DOI: 10.1124/dmd.118.081166
This article has not been copyedited and formatted. The final version may differ from this version.

Abstract

Exemestane (EXE) is an aromatase inhibitor used for the prevention and treatment of estrogen receptor-positive breast cancer. Although the known major metabolic pathway for EXE is reduction to form the active 17β-dihydro-EXE (17β-DHE) and subsequent glucuronidation to 17β-hydroxy-EXE-17-O-β-D-glucuronide (17β-DHE-Gluc), previous studies suggest that other major metabolites exist for exemestane. In the present study, a liquid chromatography-mass spectrometry (LC-MS) approach was used to acquire accurate mass data in MS^E mode, in which precursor ion and fragment ion data was obtained simultaneously to screen novel phase II EXE metabolites in urine specimens from women taking EXE. Two major metabolites predicted to be cysteine conjugates of EXE and 17β-DHE by elemental composition were identified. The structures of the two metabolites were confirmed to be 6-methylcysteinylandrosta-1,4-diene-3,17-dione (6-EXE-cys) and 6-methylcysteinylandrosta-1,4-diene-17β-hydroxy-3-one (6-17β-DHE-cys) after comparison to their chemically-synthesized counterparts. Both underwent biosynthesis *in vitro* in three stepwise enzymatic reactions with the first involving glutathione conjugation. The cysteine conjugates of EXE and 17β-DHE were subsequently quantified by LC-MS in the urine and matched plasma samples of 132 subjects taking EXE. The combined 6-EXE-cys plus 6-17β-DHE-cys made up 77% of total EXE metabolites in urine (versus 1.7, 1.4, and 21% for EXE, 17β-DHE, and 17β-DHE-Gluc, respectively) and 35% in plasma (versus 17, 12, and 36% for EXE, 17β-DHE, and 17β-DHE-Gluc, respectively). Therefore, cysteine conjugates of EXE and 17β-DHE appear to be major metabolites of EXE in both urine and plasma.

Downloaded from dmd.aspetjournals.org at ASPET Journals on April 19, 2024

DMD Fast Forward. Published on September 26, 2018 as DOI: 10.1124/dmd.118.081166
This article has not been copyedited and formatted. The final version may differ from this version.

Introduction

Breast cancer is the most frequently diagnosed cancer in the USA. (Howlader et al., 1975-2013) An estimated 252,710 new cases of female breast cancer were diagnosed in the USA in 2017 with approximately 75% of these being estrogen receptor-positive (ER+). (Osborne and Schiff, 2011; Siegel et al., 2017) In post-menopausal women, treatment for early-stage ER+ breast cancer has been focused primarily on the elimination of estrogen-induced tumor cell growth. Aromatase inhibitors (AIs) like the steroidal substrate analog, exemestane (EXE), act to inhibit aromatase activity by blocking the biosynthesis of estrone and estradiol, thereby preventing estrogen-induced tumor cell growth. (Miller, 1999; Campos, 2004; Santen et al., 2009) Clinical trials have shown that the use of AIs increases disease-free survival and decreases the occurrence of contralateral breast cancer as compared to the use of selective estrogen receptor modulators like tamoxifen. (Howell et al., 2005; Ferretti et al., 2006; Arimidex et al., 2008; Eisen et al., 2008) EXE is widely used for the adjuvant treatment and prevention of breast cancer in postmenopausal women. (Wang and Chen, 2006; Hong et al., 2007; Deeks and Scott, 2009; Petkov et al., 2009) While AIs like EXE represent an improvement in treatment and prevention of breast cancer, considerable inter-individual variation exists in patients' response to these drugs. (Paridaens et al., 2003; Chia et al., 2008; Campos et al., 2009; Gluck, 2010) The causes for this inter-individual variability have not been clearly elucidated.

Phase I metabolites of EXE had been identified *in vivo*. In addition to the major active phase I metabolite, 17β-hydroxy (OH)-EXE (17β-DHE), several minor metabolites with much lower activities are formed including 6ξ-hydroxy-6ξ-hydroxymethylandrosta-1,4-diene-3,17-dione, 6ξ-hydroxyandrosta-1,4-diene-3,17-dione, 3ξ-hydroxy-5ξ-androst-1-ene-6-methylene-

Downloaded from dmd.aspetjournals.org at ASPET Journals on April 19, 2024

DMD Fast Forward. Published on September 26, 2018 as DOI: 10.1124/dmd.118.081166
This article has not been copyedited and formatted. The final version may differ from this version.

17-one, 6ξ-17β-dihydroxy-6ξ-hydroxymethylandrosta-1,4-diene-3-one and 6ξ-17β-dihydroxyandrosta-1,4-diene-3-one. (Evans et al., 1992; Cavalcanti Gde et al., 2011; de Albuquerque Cavalcanti et al., 2011) Cytosolic aldo-keto reductase 1Cs and carbonyl reductase 1 are highly active in EXE reduction to 17β-DHE *in vitro* and several common variants in the cytosolic keto steroid reductases were associated with altered enzymatic activity *in vitro*. (Platt et al., 2016; Peterson et al., 2017) Multiple hepatic monoxygenases from Cytochrome P450 (CYP450) families 1, 2, and 3 were confirmed to catalyze the production of 6-hydroxymethylandrosta-1,4,6-triene-3,17-dione, 17α-DHE, as well as the active metabolite 17β-DHE. (Peterson et al., 2017) CYP4A11 was also found to be responsible for formation of 17β-DHE, while CYP3A was active in EXE oxidation to form 6-hydroxymethylexemestane. (Kamdem et al., 2011)

UGT2B17 is the major enzyme responsible for the glucuronidation of 17β-DHE, and the *UGT2B17* deletion polymorphism was linked to increased levels of 17β-DHE formation in plasma of women taking EXE. (Sun et al., 2010; Luo et al., 2017) Interestingly, while drastic decreases in 17β-DHE-Gluc levels (e.g., up to 29-fold in plasma) were associated with increasing numbers of the *UGT2B17* deletion allele in women taking EXE, only a small (1.3-fold) increase in plasma 17β-DHE was observed in the same women. (Luo et al., 2017) This suggests that other metabolic or excretion pathways may also play a role in EXE metabolism.

The goal of the present study was to characterize other major phase II metabolites of EXE. Results are presented demonstrating the existence of novel phase II cysteine conjugate EXE metabolites in both the urine and plasma from women taking EXE.

Downloaded from dmd.aspetjournals.org at ASPET Journals on April 19, 2024

DMD Fast Forward. Published on September 26, 2018 as DOI: 10.1124/dmd.118.081166
This article has not been copyedited and formatted. The final version may differ from this version.

Materials and Methods

Chemicals and materials. EXE was purchased from Sigma-Aldrich (St Louis, MO, USA). 17β-DHE, 17β-OH-EXE-17-O-β-D-glucuronide (17β-DHE-Gluc), 17β-OH-EXE-d3 (D_3-17β-DHE), 17β-OH-EXE-d3-17-O-β-D-glucuronide (D_3-17β-DHE-Gluc) and EXE-19-d3 (D_3-EXE) were purchased from Toronto Research Chemicals (North York, ON, Canada). Ammonium formate was obtained from Sigma-Aldrich (St Louis, MO, USA) while ammonium acetate and formic acid were purchased from Thermo-Fisher Scientific (Waltham, MA, USA). Acetonitrile was purchased from Merck (Kenilworth, NJ, USA). Solvent and buffer modifiers for ultra-pressure liquid chromatography-mass spectrometry (UPLC-MS) analysis including acetonitrile, ammonium formate, ammonium acetate and formic acid were all LC-MS grade. Milli-Q water was used for the preparation of all solutions. Pooled human liver cytosol (HLC; mixed gender, pool of 50 subjects) was purchased from XENOTECH (Kansas City, KS, USA). Reduced L-glutathione (GSH)- and glutamyltranspeptidase (γ-GT) from equine kidney were purchased from Sigma-Aldrich (St Louis, MO, USA). L-Cysteine was purchased from Alfa Aesar (Heysham, Lancashire, UK). Preparative C-18 thin layer chromatography (TLC) plates (20cm ×20cm ×1mm) were obtained from Sigma Aldrich (St Louis, MO, USA). Hexane, diethyl ether, acetonitrile, potassium hydroxide and methanol used for chemical synthesis were of ACS or higher quality and were purchased from VWR (Radnor, PA, USA).

Subjects and samples. One hundred and thirty-two post-menopausal breast cancer patients (1 Hispanic, 2 African-Americans, 2 Asians and 127 Caucasians; age range: 35 to 89 y) with ER+ breast tumors were recruited into this study from the Breast Oncology Clinic at the Penn State Hershey Cancer Institute. Approval was obtained from the Institutional Review

Downloaded from dmd.aspetjournals.org at ASPET Journals on April 19, 2024

DMD Fast Forward. Published on September 26, 2018 as DOI: 10.1124/dmd.118.081166
This article has not been copyedited and formatted. The final version may differ from this version.

Board at Penn State University with informed consent obtained from all subjects. Subjects took a single pill (25 mg) of EXE daily (orally) for at least 28 consecutive days and provided blood (10 mL) and urine (up to 50 mL) specimens at between 4 to 6 h after pill ingestion as described previously. (Luo et al., 2017) Blood was separated by centrifugation at 1300 g for 15 min at room temperature. Aliquoted plasma and buffy coat fractions of blood samples and aliquoted urine samples were stored at −80°C until analysis. As a control for EXE metabolism, specimens obtained from women not taking EXE that were recruited into other studies at Penn State University College of Medicine (Hershey, PA; n=10) were also examined to exclude false positives. (Ashmore et al., 2013)

Sample preparation for identification of EXE metabolites. Ten urine specimens from subjects taking EXE and 10 urine specimens from control subjects who did not take EXE were selected for analysis. One hundred µL of 100% methanol was added to a 50 µL aliquot of each urine sample to extract EXE and its metabolites. After vortexing and subsequent centrifugation at 16,100 × g for 10 min at 4°C, the supernatant was transferred to a fresh sample vial for analysis by UPLC-MS.

UPLC-MS conditions for screening of EXE metabolites in urine. For the simultaneous identification of potential novel phase II metabolites and analysis of known metabolites (including EXE, 17β-DHE and 17β-DHE-Gluc), urine samples were prepared as described above and analyzed using a UPLC-MS system (Waters) consisting of an Acquity UPLC pump, an Acquity sample manager-FTN, an ACQUITY UPLC BEH column C18 (2.1X100 mm, 1.7 µm particle size), and a XEVO G2-S QTOF mass spectrometer. UPLC was performed at a flow rate of 0.4 mL/min with solvent A (5 mM ammonium formate and 0.01%

Downloaded from dmd.aspetjournals.org at ASPET Journals on April 19, 2024

DMD Fast Forward. Published on September 26, 2018 as DOI: 10.1124/dmd.118.081166
This article has not been copyedited and formatted. The final version may differ from this version.

formic acid in water) and solvent B (100% acetonitrile) using the following conditions for urine specimens: 0.5 min at 25% solvent B, a linear gradient to 100% solvent B in 4 min, 1.5 min at 100% solvent B, followed by re-equilibrium with 25% solvent B for 2 min. The injection volume of each prepared urine sample was 2 µL. The column temperature was 35°C. The Waters XEVO G2-S QTOF MS was equipped with an electrospray ionization probe operated in the positive-ion mode, with a capillary voltage at 0.6 kV. Nitrogen was used as both the cone and desolvation gases with flow rates maintained at 50 and 800 L/h, respectively. Ultra-pure argon was used as the collision gas with a flow rate of 0.1 L/h. The source and desolvation gas temperatures were 120 and 500°C, respectively, and the dwell time for each ion was 300 msec. The mass spectrometer was operated in MS^E mode (MassLynx, Waters) as a non-targeted method for metabolite identification. (Plumb et al., 2006) In this method, two interleaved scan functions were used for data acquisition with both functions collecting data over the same mass range [$(m/z)^+$ = 50-1250]. The first scan acquired data using a low collision energy and collected information on the intact (parent) ions in each sample. The second scan acquired data with ramped collision energy from low to high and collected the fragment (daughter) ion data of the ions in the preceding scan. (Bateman et al., 2007)

Chemical synthesis of 6-methylcysteinylandrosta-1,4-diene-3,17-dione and 6-methylcysteinylandrosta-1,4-diene-17β-hydroxy-3-one. The EXE and 17β-DHE used for the chemical synthesis of **6-methylcysteinylandrosta-1,4-diene-3,17-dione (**6-EXE-cys) and **6-methylcysteinylandrosta-1,4-diene-17β-hydroxy-3-one (**6-17β-DHE-cys) were synthesized as previously described. (Platt et al., 2016) Nuclear magnetic resonance (NMR) spectra was recorded with a Bruker Avance I instrument with 500 MHz for hydrogen and 125

Downloaded from dmd.aspetjournals.org at ASPET Journals on April 19, 2024

DMD Fast Forward. Published on September 26, 2018 as DOI: 10.1124/dmd.118.081166
This article has not been copyedited and formatted. The final version may differ from this version.

MHz for carbon. Chemical shifts were measured based on the residual protium in NMR solvent and product purity was determined by UPLC spectrum monitored at 254 nm.

(i) 6-EXE-cys. EXE (8.0 mg, 0.027 mmol) and L-cysteine (9.7 mg, 0.080 mmol) were added to a 10 mL round-bottom flask under the protection of argon, followed by addition of degassed 1.25 N potassium hydroxide in 25% methanol (1 mL). The mixture was stirred at ambient temperature for 24 h and the pH was then adjusted to 5.0 with 2 N cold HCl. The reaction mixture was subsequently applied on a preparative C-18 reverse phase TLC developing in a chamber containing 20% acetonitrile in water. The product band determined by 254 nm UV visualization at Rf = 0.3 was scratched off from the TLC plate with a spatula into a clean 100 mL round-bottom flask. Pure methanol (40 mL) was added to extract the product. After filtration of the methanol-extracted mixture through a fritted funnel and flushed with methanol, the solvent was removed by a rotary evaporator. The residue was washed with 100% hexane (2 × 1 mL) and 100% diethyl ether (2 × 1 mL), and dried to afford the product (1.5 mg, Y = 13%) as an off-white semisolid. ^{1}H NMR (CD_3OD) δ 7.31 (d, J = 10.2 Hz, 1 H), 6.23 (dd, J_1 = 10.2 Hz, J_2 = 1.8 Hz, 1 H), 6.12 (m, 1 H), 3.71 (m, 1 H), 3.16-3.19 (m, 1 H), 2.93-3.03 (m, 2 H), 2.83 (m, 1 H), 2.73 (m, 1 H), 2.46 (m, 1 H), 2.35 (m, 1 H), 1.95-2.12 (m, 3 H), 1.88 (m, 1 H), 1.64-1.84 (m, 3 H), 1.25-1.39 (m, 3 H), 1.33 (s, 3 H), 1.06-1.12 (m, 1 H), 0.98 (s, 3 H); ^{13}C DEPT135 (CD_3OD) δ 159.6, 127.0, 122.0, 55.0, 51.2, 40.7, 39.9 (CH_2), 36.2 (CH_2), 35.9, 34.6 (CH_2), 32.1 (CH_2), 23.2 (CH_2), 22.6 (CH_2), 18.9, 14.0. The purity was >95%.

(ii) 6-17β-DHE-cys. 17β-DHE (8.4 mg, 0.028 mmol) and L-cysteine (9.9 mg, 0.082 mmol) were added to a 10 mL round-bottom flask in a reaction procedure identical to that described above for 6-methylcysteinylandrosta-1,4-diene-3,17-dione. The final residue was also washed with hexane (2 × 1 mL) and diethyl ether (2 × 1 mL), and dried to afford the product (1.5 mg, Y = 13%) as a white semisolid. ^{1}H NMR (CD_3OD) δ 7.31 (d, J = 10.2 Hz, 1 H),

Downloaded from dmd.aspetjournals.org at ASPET Journals on April 19, 2024

DMD Fast Forward. Published on September 26, 2018 as DOI: 10.1124/dmd.118.081166
This article has not been copyedited and formatted. The final version may differ from this version.

6.23 (dd, J_1 = 10.2 Hz, J_2 = 1.8 Hz, 1 H), 6.10 (m, 1 H), 3.70 (m, 1 H), 3.57 (dd, J_1 = J_2 = 8.5 Hz, 1 H), 3.17 (m, 1 H), 2.91-2.99 (m, 2 H), 2.80 (m, 1 H), 2.70 (dd, J_1 = 12.7 Hz, d_2 = 6.5 Hz, 1 H), 2.22 (ddd, J_1 = 12.4 Hz, J_2 = J_3 = 3.9 Hz, 1 H), 1.96-1.99 (m, 1 H), 1.71-1.90 (m, 4 H), 1.68 (m, 1 H), 1.63 (m, 2 H), 1.42-1.53 (m, 2 H), 1.31 (s, 3 H), 0.9-1.2 (m, 5 H), 0.83 (s, 3 H); ^{13}C DEPT135 (CD_3OD) δ 160.1, 126.8, 121.8, 81.8, 55.4 (2 C), 55.3, 51.0, 40.9 (CH_2), 40.8, 37.4 (CH_2), 36.5, 34.7 (CH_2), 30.3 (CH_2), 24.2 (CH_2), 23.6 (CH_2), 18.9, 11.4. The purity was >95%.

Biosynthesis of 6-EXE-cys, 6-17β-DHE-cys and deuterium-labeled internal standards. 6-EXE-cys, 6-17β-DHE-cys and their corresponding deuterium-labeled internal standards were biosynthesized in a 3-step process involving an initial glutathione (GSH) conjugation reaction of EXE or 17β-DHE, removal of glutamic acid from the GSH conjugates using purified active γ-GT, and subsequent removal of glycine from the cysteinylglycine conjugate using HLC as a source of dipeptidase enzyme.

(i) GSH conjugation of EXE and 17β-DHE. Pooled HLC (1 mg) was added to a reaction containing 100 mM potassium phosphate (pH = 7.4) and 250 μM EXE or 335 μM 17β-DHE in a total volume of 1 mL. The reaction mixture was pre-incubated at 37°C for 3 min prior to the addition of 50 μL of 100 mM GSH (final GSH concentration = 5 mM). (Lash et al., 1999; Zarth et al., 2015; Shi et al., 2016) After 2 h at 37°C, the reaction was stopped with an equal reaction volume of ice-cold acetonitrile and centrifuged at 16,100 × g for 10 min at 4°C. Aliquots (50 μL) of the supernatant were injected onto the ACQUITY UPLC BEH C18 column (2.1 x 100 mm, 1.7 μm particle size) for separation by UPLC. The UPLC conditions were the same as those described above for screening of EXE metabolites. Conjugate-containing fractions were collected at UPLC retention times of 0.8 - 2.0 min for the EXE-GSH conjugate or 0.5 - 2.0 min

Downloaded from dmd.aspetjournals.org at ASPET Journals on April 19, 2024

DMD Fast Forward. Published on September 26, 2018 as DOI: 10.1124/dmd.118.081166
This article has not been copyedited and formatted. The final version may differ from this version.

for the 17β-DHE-SG conjugate prior to their concentration and removal of organic solvent by speedvac.

(ii) γ-GT-mediated removal of γ-glutamyl from the GSH conjugates of EXE and 17β-DHE. The EXE-SG and 17β-DHE-GSH conjugates collected from above were digested at 37°C for 15 min with 1.0 U/mL γ-GT, 100 mM potassium phosphate (pH 7.4), 20 mM glycylglycine, and 5 mM dithiothreitol in a total volume of 600 µL as previously described. (Lash et al., 1999; Del Corso et al., 2006; Grillo et al., 2008) The reaction was stopped with an equal reaction volume of ice-cold acetonitrile and centrifuged at 16,100 × g for 10 min at 4°C, and aliquots (50 µL) of the supernatant were injected onto the same UPLC system described above. Conjugate-containing fractions were collected at UPLC retention times of 1.0-1.5 min for the EXE-cysteinylglycine conjugate and 0.5 – 1.0 min for the 17β-DHE-cysteinylglycine conjugate prior to their concentration to half their original volume by speedvac.

(iii) Dipeptidase-mediated removal of glycine from cysteinylglycine conjugates. Collected EXE-cysteinylglycine or 17β-DHE-cysteinylglycine conjugates were digested with 1.0 mg/mL pooled HLC in 100 mM potassium phosphate buffer (pH 7.4), 0.2 mM $MnCl_2$, and 5 mM dithiothreitol at 37°C in a final reaction volume of 200 µL. (Hirota et al., 1986; Josch et al., 1998; Cappiello et al., 2004; Del Corso et al., 2006) The reaction was stopped with an equal reaction volume of ice-cold acetonitrile and centrifuged at 16 100 × g for 10 min at 4°C, and aliquots (50 µL) of the supernatant were injected onto the same UPLC system described above.

(iv) Biosynthesis of D_3-6-EXE-cys and D_3-6-17β-DHE-cys. In enzymatic reactions identical to those described in steps (i) – (iii) above, D_3-EXE or D_3-17β-DHE was used as the starting material at 330 µM in 1 mL reactions. Collected D_3-6-EXE-cys and D_3-6-17β-DHE-cys conjugates were dried by speedvac and dissolved in pure methanol. The concentrations for the

Downloaded from dmd.aspetjournals.org at ASPET Journals on April 19, 2024

DMD Fast Forward. Published on September 26, 2018 as DOI: 10.1124/dmd.118.081166
This article has not been copyedited and formatted. The final version may differ from this version.

stock solutions of D_3-6-EXE-cys and D_3-6-17β-DHE-cys, estimated by comparing MS peak area with the chemically synthesized standard, were 2.5 and 10 μg/mL, respectively.

Sample preparation for quantification of EXE and its metabolites in urine and plasma. To quantify *in vivo* levels of EXE and its metabolites, the sample preparation method was modified from that described above for metabolite identification. For EXE metabolite analysis in plasma, a 2.5 μL aliquot of each plasma sample was first spiked with 2.5 μL of a mixture of deuterium-labeled internal standards in methanol [D_3-EXE (0.17 μM), D_3-17β-DHE (1.7 μM), D_3-17β-DHE-Gluc (0.52 μM), D_3-6-EXE -cys (0.06 μM) and D_3-6-17β-DHE-cys (0.25 μM)]. Twenty μL of pure methanol was then added to extract EXE and its metabolites and to precipitate proteins. After vortexing and subsequent centrifugation at 16,100 × g for 10 min at 4°C, 15 μL of the supernatant was transferred to a sample vial and mixed with 15 μL water prior to analysis by UPLC-MS.

For EXE metabolite analysis in urine, a 2.5 μL aliquot of each urine sample was first spiked with 2.5 μL of the same deuterium-labeled internal standard mixture described above. Ten μL of 75% methanol was then added to extract EXE and its metabolites. After vortexing and subsequent centrifugation at 16,100 × g for 10 min at 4°C, 10 μL of the supernatant was transferred to a sample vial and mixed with 5 μL water prior to analysis by UPLC-MS.

UPLC-MS conditions for quantification of EXE and its metabolites in urine and plasma. For the simultaneous quantification of EXE, 17β-DHE, 17β-DHE-Gluc, 6-EXE-cys, and 6-17β-DHE-cys, urine and plasma samples were prepared as described above. Using the same UPLC-MS system described above, UPLC was performed with solvent A (5 mM ammonium formate and 0.01% formic acid in water) and solvent B (100% acetonitrile) using

Downloaded from dmd.aspetjournals.org at ASPET Journals on April 19, 2024

DMD Fast Forward. Published on September 26, 2018 as DOI: 10.1124/dmd.118.081166
This article has not been copyedited and formatted. The final version may differ from this version.

the following conditions for both urine and plasma specimens: 0-1.5 min at 25% solvent B, a linear gradient to 52% solvent B for 1.5-2.5 min, 2.5-4.5 min at 52% solvent B, a linear gradient to 95% solvent B from 4.5 to 5 min, 5-9.5 min at 95% solvent B, followed by a linear gradient to initial conditions of 25% solvent B from 9.5 to 10 min. This was followed by a 10 min run at 25% solvent B to equilibrate the column to initial condition before next sample injection. The flow rate was 0.4 mL/min from 0 to 5 min, 0.8 mL/min from 5 to 9.5 min and back to 0.4 mL/min from 9.5 to 10 min. The injection volume of each prepared urine and plasma sample was 5 µL. The column temperature was 35°C. The Waters XEVO G2-S QTOF MS was operated in MS/MS mode, with the electrospray ionization probe operated in the positive-ion mode and a capillary voltage at 0.6 kV. The cone and desolvation gases flow rates were maintained at 50 and 800 L/h, respectively, and the collision gas flow rate was 0.1 L/h. The source and desolvation gas temperatures were 120 and 500°C, respectively, and the dwell time for each ion was 300 msec. The ion-related parameters for the 10 transitions monitored are listed in Table 1.

The limits of quantification for EXE, 17β-DHE, 17β-DHE-Gluc, 6-EXE-cys and 6-17β-DHE-cys were 2.1 nM, 1.6 nM, 1.2 nM, 0.7 nM and 7.2 nM, respectively, in plasma, and 2.1 nM, 1.6 nM, 6.3 nM, 1.5 nM and 7.2 nM, respectively, in urine. Standard curves were constructed by plotting the ratio of analyte peak area to peak area of the corresponding internal standard (described above) versus concentration of analyte standard. The concentrations of stock standards were 1000 ppm. A serial dilution of standards at concentrations ranging from 1.6 nM to 1.7 µM, 1.6 nM to 1.7 µM, 1.0 nM to 2.1 µM, 0.7 nM to 12 µM and 4.6 nM to 2.4 µM were used to establish standard curves for EXE, 17β-DHE, 17β-DHE-Gluc, 6-EXE-cys and 6-17β-DHE-cys, respectively. Analyte concentrations were determined by measuring the peak area ratios of analyte to internal standard and then

Downloaded from dmd.aspetjournals.org at ASPET Journals on April 19, 2024

DMD Fast Forward. Published on September 26, 2018 as DOI: 10.1124/dmd.118.081166
This article has not been copyedited and formatted. The final version may differ from this version.

calculating analyte concentration from the appropriate standard curve using Waters' TargetLynx software. Urinary creatinine was measured as previously described. (Luo et al., 2017)

Statistical analysis. Calculations of mean and standard error were performed using Prism (version 7, Graph Pad Software, San Diego, CA, USA).

Downloaded from dmd.aspetjournals.org at ASPET Journals on April 19, 2024

DMD Fast Forward. Published on September 26, 2018 as DOI: 10.1124/dmd.118.081166
This article has not been copyedited and formatted. The final version may differ from this version.

Results

Identification of EXE and 17β-DHE conjugates. Urine specimens from subjects taking EXE were extracted and analyzed by UPLC-MS using MS^E, a non-targeted method for metabolite identification that allows for the scanning of both intact ions (channel 1) and fragment ions (channel 2) simultaneously over the same mass range.

As shown by representative chromatographs in Figure 1, the MS^E method applied in this study was sensitive enough to detect known EXE metabolites extracted from the intact ion channel 1 including EXE (panel A; extracted mass = 297.19), 17β-DHE (panel C; extracted mass = 299.20) and 17β-DHE-Gluc (panel E; extracted mass = 475.23) in the urine from subjects taking EXE. All peaks corresponded with those observed for EXE, 17β-DHE, and 17β-DHE-Gluc standards (panels B, D, and F, respectively); none were observed in the urine of subjects not taking EXE (results not shown).

In screening for novel EXE conjugates, the MS trace of $(m/z)^+ = 297.185$ for $[EXE+H]^+$, the common fragment ion for EXE conjugates, was extracted from the fragment ion channel 2 (Figure 2, panel A). In addition to the expected peak for EXE (retention time 3.20 min), two major peaks (termed Peaks 1 and 2, retention times = 1.33 and 1.74 min, respectively) were observed. Neither of these peaks were detected in urine specimens from control subjects not taking EXE (results not shown). Molecular ions for compounds that correspond to these two fragment peaks were then searched within the intact ions channel (channel 1); the retention times of Peaks 1 and 2 in the intact (parent) ion channel 1 (Figure 2, panel B) matched that observed for Peaks 1 and 2 in the fragment ion channel 2 (Figure 2, panel A). The corresponding mass spectrum of the parent ion for Peak 1 from the intact (parent) ion channel 1 showed a major peak with a $(m/z)^+ = 418.2060$, presumably the $[X+H]^+$ ion, where 'X' refers to an unknown EXE conjugate (Figure 2, panel C). Two additional accurate mass peaks were

Downloaded from dmd.aspetjournals.org at ASPET Journals on April 19, 2024

DMD Fast Forward. Published on September 26, 2018 as DOI: 10.1124/dmd.118.081166
This article has not been copyedited and formatted. The final version may differ from this version.

observed (Figure 2, panel C), with $(m/z)^+$ = 440.1874 and 456.1615, likely corresponding to the $(m/z)^+$ for $[X+Na]^+$ and $[X+K]^+$, respectively. The accurate mass spectrum for Peak 2 (data not shown) was identical to that observed for Peak 1 (Figure 2, panel C), suggesting that the two peaks are isomers of the same EXE conjugate. The trace of 418.206 extracted from the intact (parent) ion scan from channel 1 (from Figure 2, panel C) exhibited two peaks (Figure 2, panel D) that matched the retention times of peaks 1 and 2 extracted from fragment ion channel 2 for $(m/z)^+$ = 297.185 (Figure 2, panel A). Peak 1 was observed in all 10 urine specimens screened by MS^E, while Peak 2 was detected in 7 of the 10 urine specimens.

The potential composition for the parent ion of $(m/z)^+$ = 418.2057 was calculated using the Elemental Composition tool within MassLynx 4.1. Since the composition of EXE is $C_{20}H_{24}O_2$, the molecular composition of possible EXE conjugates had to contain $\geq$ 20 carbons and $\geq$ 2 oxygens. The only candidate composition available that matched these criteria was $C_{23}H_{32}NO_4S$ [$(m/z)^+$ = 418.2052], which matched exactly with the predicted structure corresponding to the cysteine conjugate of EXE. Therefore, compounds responsible for Peaks 1 and 2 in the urine of women taking EXE were predicted to be EXE-cys isomers ($C_{23}H_{31}NO_4S$).

For identifying conjugates of 17β-DHE, an approach similar to that used for identifying EXE conjugates was undertaken. A trace corresponding to $(m/z)^+$ = 299.201 for [17β-DHE $+H]^+$, the common fragment ion for 17β-DHE conjugates, was extracted from the fragment ion channel 2 (Figure 3, panel A) while a trace which corresponding to the intact (parent) ion for 17β-DHE-cys [$(m/z)^+$ = 420.221] was extracted from the intact (parent) ion channel 1 (Figure 3, panel B). Two fragment ion peaks were observed in the channel 2 trace (Peak 3 at 0.86 min and Peak 4 at 1.23 min; Figure 3, panel A) that aligned exactly with the retention times of peaks extracted from the intact (parent) ion [$(m/z)^+$ = 420.2209] trace in channel 1 (Figure 3,

Downloaded from dmd.aspetjournals.org at ASPET Journals on April 19, 2024

DMD Fast Forward. Published on September 26, 2018 as DOI: 10.1124/dmd.118.081166
This article has not been copyedited and formatted. The final version may differ from this version.

panel B). The mass spectrum extracted for Peak 3 from the intact (parent) ion channel 1 is shown in Figure 3, panel C. The peaks of $(m/z)^+$ = 420.2209, 442.2027 and 458.1770 likely corresponded to the ions of $[17\beta\text{-DHE-cys} + H]^+$, $[17\beta\text{-DHE-cys} + Na]^+$ and $[17\beta\text{-DHE-cys} + K]^+$, respectively. Similar to that observed for EXE-cys conjugates, Peak 3 was observed in all 10 urine samples screened by the MS^E, while Peak 4 was observed in 7 of the 10 urine samples. Again, neither of these peaks were detected in urine samples from control subjects not taking EXE (results not shown). Therefore, compounds responsible for Peaks 3 and 4 were predicted to be 17β-DHE-cys isomers ($C_{23}H_{33}NO_4S$).

Chemical synthesis of cysteine conjugates of EXE and 17β-DHE. To confirm the structures of the predicted cysteine conjugates of EXE and 17β-DHE identified above, 6-EXE-cys and 6-17β-DHE-cys were synthesized chemically. As described in the Materials and Methods, the structure of both chemically-synthesized cysteine conjugates were confirmed by NMR and the purity of both conjugates was confirmed by LC-MS to be >95% (results not shown).

The retention times for peaks corresponding to chemically-synthesized 6α-EXE-cys and 6α-17β-DHE-cys (Figure 4, panels A and B, respectively) matched those observed for the predicted EXE-cys and 17β-DHE-cys Peaks 1 and 3, respectively (Figure 2, panel D and Figure 3, panel B, respectively) detected in the urine of subjects taking EXE. In addition, co-elution experiments were performed by adding chemically-synthesized 6α-EXE-cys and 6α-17β-DHE-cys into urine specimens of EXE-treated subjects. LC-MS analysis showed increases in peak size for each compound (results not show), further demonstrating that the urinary peaks are identical to the chemically-synthesized standards. Together, these data

Downloaded from dmd.aspetjournals.org at ASPET Journals on April 19, 2024

DMD Fast Forward. Published on September 26, 2018 as DOI: 10.1124/dmd.118.081166
This article has not been copyedited and formatted. The final version may differ from this version.

suggest that the MS Peaks 1 and 3 (Figure 2, panel D and Figure 3, panel B, respectively) from urine of women taking EXE corresponded to 6α-EXE-cys and 6α-17β-DHE-cys.

Biosynthesis of cysteine conjugates of EXE and 17β-DHE. GSH is a tripeptide (γ-glu-cys-gly) that can conjugate to an electrophilic substrate, which can be further metabolized to form cysteine conjugates during mercapturic acid biosynthesis. (Hinchman and Ballatori, 1994; van Bladeren, 2000; Hayes et al., 2005) To explore whether this mechanism of cysteine conjugate formation may be occurring for EXE and 17β-DHE *in vivo*, cysteine conjugates of EXE and 17β-DHE were enzymatically synthesized in a 3-step reaction. For the synthesis of EXE-cys, the EXE-glutathione conjugate was first synthesized by incubating EXE with GSH in the presence of HLC as a source of glutathione-*S*-transferases (GSTs). Products of the reaction were analyzed by LC-MS. Three peaks (retention times = 1.15, 1.60 and 1.81 min) were detected as potential EXE-glutathione conjugates [$(m/z)^+ = 604.27$; results not shown]. Using LC-purified peak 1 (retention time = 1.15 min), EXE-cys conjugates were then formed (Figure 4, panel C) after two additional reactions using purified γ-GT in reaction 1 and then HLC for reaction 2. The retention time observed for the enzymatically-synthesized EXE-cys conjugate (1.31 min) was similar to that observed for the chemically-synthesized 6-EXE-cys conjugate (1.33 min; Figure 4, panel A) and was similar to that observed for the putative 6-EXE-cys conjugate corresponding to Peak 1 in the urine of subjects taking EXE (Figure 2, panel D).

Using 17β-DHE as substrate, a similar 3-step reaction approach was performed to enzymatically synthesize the 6-17β-DHE-cys conjugate. The retention time observed for the enzymatically-synthesized 6-17β-DHE-cys conjugate (0.84 min; Figure 4, panel D) was similar to that observed for the chemically-synthesized 6-17β-DHE-cys conjugate (Figure 4, panel B)

Downloaded from dmd.aspetjournals.org at ASPET Journals on April 19, 2024

DMD Fast Forward. Published on September 26, 2018 as DOI: 10.1124/dmd.118.081166
This article has not been copyedited and formatted. The final version may differ from this version.

and to that observed for the putative 17β-DHE-cys conjugate corresponding to Peak 3 in the urine of subjects taking EXE (Figure 3, panel B). In addition, a similar pattern was observed for both the enzymatically-synthesized D_3-labeled 6-EXE-cys and 6-17β-DHE-cys conjugates (Figure 4, panels E and F, respectively). All cysteine conjugates were confirmed by analysis of corresponding mass spectra (results not shown).

Quantification of EXE and its metabolites *in vivo.* For quantification of EXE and its metabolites *in vivo*, EXE metabolites were analyzed by UPLC-MS/MS for all urine samples and matched plasma samples from 132 post-menopausal breast cancer patients who had taken 25mg EXE per day for at least 4 weeks. As shown for representative MS chromatograms of EXE metabolites from a subject taking EXE (Figure 5), the retention times were 4.02 min for EXE, 3.73 min for 17β-DHE, 2.65 min for 17β-DHE-Gluc, 1.34 min for 6α-EXE-cys and 0.88 min for 6α-17β-DHE-cys for both urine and plasma using this UPLC-MS/MS method. In all cases, the retention times of each peak was similar to that of their corresponding internal standard peaks (see Figure's 1 and 4). While the predicted isomers of EXE-cys and 17β-DHE-cys (Peaks 2 and 4 in Figure 2, panel D and Figure 3, panels B, respectively) were not quantified due to a lack of accurate standards, they may be present at similar or higher levels than that observed for 6-EXE-cys and 6-17β-DHE-cys if their MS response factors are similar to 6-EXE-cys and 6-17β -DHE-cys, respectively.

The major metabolites in the plasma of subjects treated with EXE were 17β-DHE-Gluc (mean = 30 nM; Table 2) and 6α-EXE-cys (mean = 22 nM). The levels of 6-17β-DHE-cys (5.9 nM) and 17β-DHE (2.5 nM) were lower than that observed for the parent EXE (mean = 14 nM) in plasma, with the average percentage of 17β-DHE in total quantified EXE metabolites (TEM) observed at 3-fold lower levels than that observed for 17β-DHE-Gluc. The mean levels of the

Downloaded from dmd.aspetjournals.org at ASPET Journals on April 19, 2024

DMD Fast Forward. Published on September 26, 2018 as DOI: 10.1124/dmd.118.081166
This article has not been copyedited and formatted. The final version may differ from this version.

combined cysteine conjugates for plasma EXE plus 17β-DHE was roughly equivalent to the levels of plasma 17β-DHE-Gluc, with the average percent of TEM ranging from 35-36% for both (6-EXE-cys + 6-17β-DHE-cys) and 17β-DHE-Gluc. The percent of 17β-DHE-Gluc and 6-EXE-cys in TEM (36% and 23%, respectively) were highest when compared to other EXE metabolites in the plasma of EXE-treated subjects, ranging from 12% to 17% for 17β-DHE, 6-17β-DHE-cys and EXE.

While a similar trend was observed for urinary EXE metabolites, the levels of urinary 17β-DHE-Gluc was 5.5-fold less than the combined cysteine conjugates for urinary EXE plus 17β-DHE, which were the major urinary metabolites in women taking EXE (Table 2). 17β-DHE-Gluc comprised, on average, 21% of total quantified urinary EXE metabolites versus the combined 6-EXE-cys plus 6-17β-DHE-cys conjugates, which comprised 79% of total quantified urinary EXE metabolites. The levels of urinary 17β-DHE-Gluc (1.4 nmol/mg creatinine) were slightly lower than that observed for 6-17β-DHE-cys (1.8 nmol/mg creatinine), which was 3.3-fold lower than that observed for the major urinary metabolite, 6-EXE-cys. The mean levels of urinary 6-EXE-cys (mean = 5.9 nmol/mg creatinine) was almost 900-fold higher than the urinary metabolite observed at the lowest level, 17β-DHE (mean = 0.0066 nmol/mg creatinine).

Downloaded from dmd.aspetjournals.org at ASPET Journals on April 19, 2024

DMD Fast Forward. Published on September 26, 2018 as DOI: 10.1124/dmd.118.081166
This article has not been copyedited and formatted. The final version may differ from this version.

Discussion

Previous studies indicated that the major mode of metabolism of EXE is by reduction to form 17β-DHE and UGT2B17-mediated glucuronidation to form 17β-DHE-Gluc. (Sun et al., 2010; Luo et al., 2017) In the present study, two novel major EXE metabolites were identified – the cysteine conjugates of EXE (6-EXE-cys) and 17β-DHE (6-17β-DHE-cys). The mean levels of the combined 6α-EXE-cys plus 6α-17β-DHE-cys were 5.5-fold higher than that observed for 17β-DHE-Gluc in urine and were similar to the levels of 17β-DHE-Gluc observed in plasma. 6-EXE-cys formed the major cysteine conjugate of EXE, comprising 77 and 79% of the total mean cysteine conjugate levels in urine and plasma, respectively. This suggests that the formation of cysteine conjugates is the major excretion pathway for EXE in humans, with 6-EXE-cys the major urinary EXE metabolite (see Scheme 1).

While the stereochemistry at the 6-position was not assigned in the current paper, we speculate the stereo orientation for the 6 substitute is "α" for both synthesized 6-EXE-cys and 6-17β-DHE-cys based on the proton coupling constant between the proton at the 4-position and the proton at the 6-position of both EXE-cys and 17β-DHE-cys conjugates. For 6-substituted steroids, long distance coupling between H-4 and H-6 in ^{1}H NMR will be observed only when the 6-substituent is in the α position. (Chin and Warren, 1972; Schneider et al., 1973; Numazawa and Oshibe, 1994; Numazawa and Yamaguchi, 1998; Gorlitzer et al., 2006). In an analysis of a series of 6-substituted phenylaliphatic steroids, Numazawa and Yamaguchi demonstrated that proton coupling between the hydrogens at the 4- and 6-positions was only observed for the 6α-substituted but not the 6β-substituted phenylaliphatic steroids.[32] Similar C-4 proton signals have been reported for a series of 6-alkyl-, 6-bromo-, and 6-(bromoacetoxy)androstenediones. (Numazawa and Oshibe, 1994; Numazawa and

Downloaded from dmd.aspetjournals.org at ASPET Journals on April 19, 2024

DMD Fast Forward. Published on September 26, 2018 as DOI: 10.1124/dmd.118.081166
This article has not been copyedited and formatted. The final version may differ from this version.

Yamaguchi, 1998) In addition, the EXE derivative, 6α-chlormethylandrosta-1,4-dien-3,17-dion, exhibits similar long distance coupling between H-4 and H-6. (Gorlitzer et al., 2006) These data are consistent with the proton coupling pattern observed by ^{1}H-NMR in the present study of 6-EXE-cys and 6-17β-DHE-cys (results not shown), suggesting that both conjugates were in the 'α'-position. However, X-ray crystallography analysis of the two conjugates will provide a more definitive validation of their structure.

Previous *in vitro* studies in a panel of human liver microsomes demonstrated that deletion of the UGT2B17 gene resulted in significant decreases in 17β-DHE-Gluc formation. (Sun et al., 2010) While drastic decreases in urinary and plasma 17β-DHE-Gluc levels were also associated with increasing numbers of the *UGT2B17* deletion allele in women taking EXE (e.g., up to 29-fold in plasma), only a small (1.3-fold) corresponding increase in plasma 17β-DHE was observed in the same women. (Luo et al., 2017) In the present study, 17β-DHE-Gluc was demonstrated to comprise 36% of the total quantified EXE metabolites in plasma, levels that were approximately equal to that observed for both of the cysteine conjugates combined (which comprised 35% of total quantified plasma EXE metabolites) and only slightly more than that observed for 6α-EXE-cys alone (which comprises 23% of total quantified plasma EXE metabolites). In addition, 17β-DHE-Gluc comprised only 21% of the total quantified EXE metabolites in urine. These values correspond with the fact that either no alterations or only small increases in urinary or plasma EXE and 17β-DHE were observed in subjects taking EXE that were homozygous for the UGT2B17 deletion polymorphism (i.e., with no active UGT2B17) in previous studies. (Luo et al., 2017)

A three-step metabolism pathway similar to the first three steps of the mercapturic acid synthesis pathway was shown to be a viable *in vivo* mechanism of EXE and 17β-DHE cysteine

Downloaded from dmd.aspetjournals.org at ASPET Journals on April 19, 2024

DMD Fast Forward. Published on September 26, 2018 as DOI: 10.1124/dmd.118.081166
This article has not been copyedited and formatted. The final version may differ from this version.

conjugate formation in the present studies. The three steps include an initial GSH conjugation reaction catalyzed by GSTs to form EXE-GSH or 17β-DHE-GSH, a second reaction catalyzed by γ-GT to remove the glutamyl moiety from the glutathione conjugate to form EXE-cysteinylglycine or 17β-DHE-cysteinylglycine, and a final reaction where the glycyl moiety is removed by dipeptidase to form the EXE-cys or 17β-DHE-cys conjugates.

In addition to the identified 6-EXE-cys (Peaks 1 in Figure 2D) and 6-17β-DHE-cys conjugates (Peaks 3 in Figure 3B), secondary peaks likely corresponding to EXE-cys (Peaks 2 in Figure 2D) and 17β-DHE-cys isomers (Peaks 4 in Figure 3B) of unknown structure were observed in the urine of women taking EXE in the present study. EXE and 17β-DHE are α-β unsaturated ketones with several double bonds for GSH conjugation. Therefore, there are several possible positions for the initial GSH conjugation step to occur. Chemical synthesis of other potential isomers of EXE-cys and 17β-DHE-cys conjugates is currently underway to confirm their structures.

Similar to phase II metabolism by glucuronidation, GSH conjugation of either EXE or 17β-DHE likely increases their rate of excretion and eliminates their anti-aromatase activities. Significant variations in levels of 6-EXE-cys and 6-17β-DHE-cys were observed in the urine and plasma samples of the 132 subjects. As shown in Table 2, 6-EXE-cys and 6-17β-DHE-cys ranged from 0.020 to 226 and 0 to 31 nM, respectively, in plasma, and from 0.0033 to 50 and 0.0033 to 10 nM, respectively, in urine. Interestingly, both the unidentified EXE cysteine conjugate isomer (Peaks 2 in Figure 2D) and the unidentified 17β-DHE cysteine conjugate isomer (Peak 4 in Figure 3B) were observed in the urine of only 7 of the 10 subjects examined in this study. There is significant genetic variability in the GST enzymes, (Hayes et al., 2005) including common copy number variants observed for both GSTM1 and GSTT1. (Seidegard et al., 1990; Bell et al., 1993; Arruda et al., 1998; Bailey et al., 1998; Roth et al., 2000; Hayes et

Downloaded from dmd.aspetjournals.org at ASPET Journals on April 19, 2024

DMD Fast Forward. Published on September 26, 2018 as DOI: 10.1124/dmd.118.081166
This article has not been copyedited and formatted. The final version may differ from this version.

al., 2005) The frequencies of homozygous deletion genotypes of GSTM1 and GSTT1 are about 50% and 14% in Caucasians, and the homozygous deletion genotypes of both GSTM1 and GSTT1 were reported to be associated with risk for a variety of cancers and may be linked to alterations in drug metabolism. (Hengstler et al., 1998) For example, GSTs are involved in the metabolism of azathioprine (AZA) to mercaptopurine, with 6-methylmercaptopurine riboside a major metabolite of mercaptopurine. The levels of 6-methylmercaptopurine riboside were two-fold lower in AZA users exhibiting the GSTM1-null genotype than AZA users carrying one or two copies of GSTM1. (Broekman et al., 2017) The deletion of GSTM1 was also associated with reduced response to AZA therapy. (Stocco et al., 2014) This suggests that if such GSTs are similarly involved in the metabolism of EXE, copy number variants or other functional polymorphisms could potentially play an important role in the metabolism and efficacy of EXE. While functional polymorphisms in both the γ-GT and dipeptidase enzymes could similarly modify the levels of EXE-cys or 17β-DHE-cys observed in the plasma and/or urine of subjects taking EXE, they are not metabolizing the functional parent compound, EXE, or its major active metabolite, 17β-DHE, and are therefore less likely to be important in overall patient response to EXE.

As described above, quantification of EXE-cys and 17β-DHE-cys conjugates was performed only for peaks corresponding to the known 6-cysteine conjugates (Peaks 1 and 3 in Figure 2D and 3B, respectively). Although their structure is presently unknown, other peaks corresponding to other EXE-cys and 17β-DHE-cys isomers were identified in the present study, potentially at levels similar to or higher than those observed for 6-EXE-cys and 6-17β-DHE-cys. Therefore, these conjugates likely comprise an even larger proportion of EXE metabolites in the urine and plasma of women taking EXE, further increasing the importance of cysteine conjugate formation and decreasing the overall importance of glucuronidation in the

Downloaded from dmd.aspetjournals.org at ASPET Journals on April 19, 2024

DMD Fast Forward. Published on September 26, 2018 as DOI: 10.1124/dmd.118.081166
This article has not been copyedited and formatted. The final version may differ from this version.

metabolism of EXE. In addition, this further supports previous results demonstrating only small changes in plasma 17β-DHE and no change in urinary 17β-DHE in subjects deficient in DHE glucuronidation capacity since the glucuronide comprises a relatively low percentage of EXE metabolites *in vivo*. (Luo et al., 2017)

A potential limitation of the present study was that the study subjects examined were primarily Caucasians (only 5 non-Caucasians out of 132 female subjects). While we did not find observable differences in the levels of EXE or its metabolites between the Caucasian subjects and the 5 non-Caucasian subjects examined in this study, it is possible that the patterns observed for Caucasian females may not be 100% generalizable to all populations. Additional studies of EXE metabolism in other racial groups will be necessary to better examine this. Another potential limitation of the current study was that the intermediate products of the first and second steps for the proposed three-step pathway for EXE-cys and 17β-DHE-cys formation were not detected in urine samples, suggesting that they are at low levels if present. This also suggests that the final two intermediate enzymatic reaction steps with γ-glutamyl transferase and cysteinylglycine dipeptidase to form the EXE-cys and 17β-DHE-cys conjugates are highly efficient.

In conclusion, two novel EXE Phase II metabolites were identified *in vivo* in women taking EXE. The two metabolites - cysteine conjugates of EXE and 17β-DHE – are the major metabolites of EXE found in the urine of subjects taking EXE, comprising, on average, 77% of total quantified urinary EXE metabolites, and were at levels similar to that observed for the other major EXE metabolite, 17β-DHE-Gluc, in the plasma of the same subjects. While their exact structure is presently unknown, other EXE and 17β-DHE cysteine conjugates were also identified, further supporting cysteine conjugate formation as the major metabolism pathway

Downloaded from dmd.aspetjournals.org at ASPET Journals on April 19, 2024

DMD Fast Forward. Published on September 26, 2018 as DOI: 10.1124/dmd.118.081166
This article has not been copyedited and formatted. The final version may differ from this version.

for EXE *in vivo*. The pathways involved in EXE-cys or 17β-DHE-cys formation could therefore potentially play an important role in the pharmacokinetics and pharmacodynamics of EXE.

Downloaded from dmd.aspetjournals.org at ASPET Journals on April 19, 2024

DMD Fast Forward. Published on September 26, 2018 as DOI: 10.1124/dmd.118.081166
This article has not been copyedited and formatted. The final version may differ from this version.

Acknowledgments

We thank the Mass Spectrometry Core facility and the Nuclear Magnetic Resonance Core facility at Washington State University-Spokane for their help with UPLC-MS and NMR respectively.

Downloaded from dmd.aspetjournals.org at ASPET Journals on April 19, 2024

DMD Fast Forward. Published on September 26, 2018 as DOI: 10.1124/dmd.118.081166
This article has not been copyedited and formatted. The final version may differ from this version.

Authorship Contributions

Participated in research design: Luo, Chen, Truica, Lazarus

Conducted experiments: Luo, Chen, Baird, Xia

Performed data analysis: Luo, Chen, Xia

Wrote or contributed to the writing of the manuscript: Luo, Chen, Truica, Xia, Lazarus

Downloaded from dmd.aspetjournals.org at ASPET Journals on April 19, 2024

DMD Fast Forward. Published on September 26, 2018 as DOI: 10.1124/dmd.118.081166
This article has not been copyedited and formatted. The final version may differ from this version.

References

Arimidex TAoiCTG, Forbes JF, Cuzick J, Buzdar A, Howell A, Tobias JS, and Baum M (2008) Effect of anastrozole and tamoxifen as adjuvant treatment for early-stage breast cancer: 100-month analysis of the ATAC trial. *Lancet Oncol* **9:**45-53.

Arruda VR, Grignolli CE, Goncalves MS, Soares MC, Menezes R, Saad ST, and Costa FF (1998) Prevalence of homozygosity for the deleted alleles of glutathione S-transferase mu (GSTM1) and theta (GSTT1) among distinct ethnic groups from Brazil: relevance to environmental carcinogenesis? *Clin Genet* **54:**210-214.

Ashmore JH, Lesko SM, Muscat JE, Gallagher CJ, Berg AS, Miller PE, Hartman TJ, and Lazarus P (2013) Association of dietary and supplemental folate intake and polymorphisms in three FOCM pathway genes with colorectal cancer in a population-based case-control study. *Genes, chromosomes & cancer* **52:**945-953.

Bailey LR, Roodi N, Verrier CS, Yee CJ, Dupont WD, and Parl FF (1998) Breast cancer and CYPIA1, GSTM1, and GSTT1 polymorphisms: evidence of a lack of association in Caucasians and African Americans. *Cancer research* **58:**65-70.

Bateman KP, Castro-Perez J, Wrona M, Shockcor JP, Yu K, Oballa R, and Nicoll-Griffith DA (2007) MSE with mass defect filtering for in vitro and in vivo metabolite identification. *Rapid Commun Mass Spectrom* **21:**1485-1496.

Bell DA, Taylor JA, Paulson DF, Robertson CN, Mohler JL, and Lucier GW (1993) Genetic risk and carcinogen exposure: a common inherited defect of the carcinogen-metabolism gene glutathione S-transferase M1 (GSTM1) that increases susceptibility to bladder cancer. *Journal of the National Cancer Institute* **85:**1159-1164.

Broekman MM, Wong DR, Wanten GJ, Roelofs HM, van Marrewijk CJ, Klungel OH, Verbeek AL, Hooymans PM, Guchelaar HJ, Scheffer H, Derijks LJ, Coenen MJ, and de Jong DJ (2017) The glutathione transferase Mu null genotype leads to lower 6-MMPR levels in patients treated with azathioprine but not with mercaptopurine. *Pharmacogenomics J*.

Campos SM (2004) Aromatase inhibitors for breast cancer in postmenopausal women. *Oncologist* **9:**126-136.

Campos SM, Guastalla JP, Subar M, Abreu P, Winer EP, and Cameron DA (2009) A comparative study of exemestane versus anastrozole in patients with postmenopausal breast cancer with visceral metastases. *Clin Breast Cancer* **9:**39-44.

Cappiello M, Lazzarotti A, Buono F, Scaloni A, D'Ambrosio C, Amodeo P, Mendez BL, Pelosi P, Del Corso A, and Mura U (2004) New role for leucyl aminopeptidase in glutathione turnover. *Biochem J* **378:**35-44.

Cavalcanti Gde A, Garrido BC, Leal FD, Padilha MC, de la Torre X, and de Aquino Neto FR (2011) Detection of new urinary exemestane metabolites by gas chromatography coupled to mass spectrometry. *Steroids* **76:**1010-1015.

Chia S, Gradishar W, Mauriac L, Bines J, Amant F, Federico M, Fein L, Romieu G, Buzdar A, Robertson JF, Brufsky A, Possinger K, Rennie P, Sapunar F, Lowe E, and Piccart M (2008) Double-blind, randomized placebo controlled trial of fulvestrant compared with exemestane after prior nonsteroidal aromatase inhibitor therapy in postmenopausal women with hormone receptor-positive, advanced breast cancer: results from EFECT. *J Clin Oncol* **26:**1664-1670.

Chin CC and Warren JC (1972) Synthesis of 2 -, 6 -, and 6 -bromoprogesterone and study of the binding site of 20 -hydroxysteroid dehydrogenase. *Biochemistry* **11:**2720-2726.

Downloaded from dmd.aspetjournals.org at ASPET Journals on April 19, 2024

DMD Fast Forward. Published on September 26, 2018 as DOI: 10.1124/dmd.118.081166
This article has not been copyedited and formatted. The final version may differ from this version.

de Albuquerque Cavalcanti G, Carius Garrido B, Dias Leal F, Costa Padilha M, Mazzarino M, de la Torre X, Botre F, and Radler de Aquino Neto F (2011) Detection of new exemestane metabolites by liquid chromatography interfaced to electrospray-tandem mass spectrometry. *J Steroid Biochem Mol Biol* **127:**248-254.

Deeks ED and Scott LJ (2009) Exemestane: a review of its use in postmenopausal women with breast cancer. *Drugs* **69:**889-918.

Del Corso A, Cappiello M, Buono F, Moschini R, Paolicchi A, and Mura U (2006) Colorimetric coupled enzyme assay for gamma-glutamyltransferase activity using glutathione as substrate. *J Biochem Biophys Methods* **67:**123-130.

Eisen A, Trudeau M, Shelley W, Messersmith H, and Pritchard KI (2008) Aromatase inhibitors in adjuvant therapy for hormone receptor positive breast cancer: a systematic review. *Cancer Treat Rev* **34:**157-174.

Evans TR, Di Salle E, Ornati G, Lassus M, Benedetti MS, Pianezzola E, and Coombes RC (1992) Phase I and endocrine study of exemestane (FCE 24304), a new aromatase inhibitor, in postmenopausal women. *Cancer Res* **52:**5933-5939.

Ferretti G, Bria E, Giannarelli D, Felici A, Papaldo P, Fabi A, Di Cosimo S, Ruggeri EM, Milella M, Ciccarese M, Cecere FL, Gelibter A, Nuzzo C, Cognetti F, Terzoli E, and Carlini P (2006) Second- and third-generation aromatase inhibitors as first-line endocrine therapy in postmenopausal metastatic breast cancer patients: a pooled analysis of the randomised trials. *Br J Cancer* **94:**1789-1796.

Gluck S (2010) Exemestane as first-line therapy in postmenopausal women with recurrent or metastatic breast cancer. *Am J Clin Oncol* **33:**314-319.

Gorlitzer K, Bonnekessel C, Jones PG, Palusczak A, and Hartmann RW (2006) [Derivatives of exemestane--synthesis and evaluation of aromatase inhibition]. *Pharmazie* **61:**575-581.

Grillo MP, Hua F, March KL, Benet LZ, Knutson CG, and Ware JA (2008) Gamma-glutamyltranspeptidase-mediated degradation of diclofenac-S-acyl-glutathione in vitro and in vivo in rat. *Chem Res Toxicol* **21:**1933-1938.

Hayes JD, Flanagan JU, and Jowsey IR (2005) Glutathione transferases. *Annu Rev Pharmacol Toxicol* **45:**51-88.

Hengstler JG, Arand M, Herrero ME, and Oesch F (1998) Polymorphisms of N-acetyltransferases, glutathione S-transferases, microsomal epoxide hydrolase and sulfotransferases: influence on cancer susceptibility. *Recent Results Cancer Res* **154:**47-85.

Hinchman CA and Ballatori N (1994) Glutathione conjugation and conversion to mercapturic acids can occur as an intrahepatic process. *J Toxicol Environ Health* **41:**387-409.

Hirota T, Nishikawa Y, Tanaka M, Igarashi T, and Kitagawa H (1986) Characterization of dehydropeptidase I in the rat lung. *Eur J Biochem* **160:**521-525.

Hong Y, Yu B, Sherman M, Yuan YC, Zhou D, and Chen S (2007) Molecular basis for the aromatization reaction and exemestane-mediated irreversible inhibition of human aromatase. *Mol Endocrinol* **21:**401-414.

Howell A, Cuzick J, Baum M, Buzdar A, Dowsett M, Forbes JF, Hoctin-Boes G, Houghton J, Locker GY, Tobias JS, and Group. AT (2005) Results of the ATAC (Arimidex, Tamoxifen, Alone or in Combination) trial after completion of 5 years' adjuvant treatment for breast cancer. *Lancet* **365:**60-62.

Howlader N, Noone AM, Krapcho M, Miller D, Bishop K, Altekruse SF, Kosary CL, Yu M, Ruhl J, Tatalovich Z, Mariotto A, Lewis DR, Chen HS, Feuer EJ, and Cronin KA (1975-2013) SEER Cancer Statistics Review.

Downloaded from dmd.aspetjournals.org at ASPET Journals on April 19, 2024

DMD Fast Forward. Published on September 26, 2018 as DOI: 10.1124/dmd.118.081166
This article has not been copyedited and formatted. The final version may differ from this version.

Josch C, Sies H, and Akerboom TP (1998) Hepatic mercapturic acid formation: involvement of cytosolic cysteinylglycine S-conjugate dipeptidase activity. *Biochem Pharmacol* **56:**763-771.

Kamdem LK, Flockhart DA, and Desta Z (2011) In vitro cytochrome P450-mediated metabolism of exemestane. *Drug Metab Dispos* **39:**98-105.

Lash LH, Lipscomb JC, Putt DA, and Parker JC (1999) Glutathione conjugation of trichloroethylene in human liver and kidney: kinetics and individual variation. *Drug Metab Dispos* **27:**351-359.

Luo S, Chen G, Truica C, Baird CC, Leitzel K, and Lazarus P (2017) Role of the UGT2B17 deletion in exemestane pharmacogenetics. *Pharmacogenomics J*.

Miller WR (1999) Biology of aromatase inhibitors: pharmacology/endocrinology within the breast. *Endocr Relat Cancer* **6:**187-195.

Numazawa M and Oshibe M (1994) 6-Alkyl- and 6-arylandrost-4-ene-3,17-diones as aromatase inhibitors. Synthesis and structure-activity relationships. *J Med Chem* **37:**1312-1319.

Numazawa M and Yamaguchi S (1998) 6-Phenylaliphatic-substituted androst-4-ene-3,17-diones as aromatase inhibitors: structure-activity relationships. *J Steroid Biochem Mol Biol* **67:**41-48.

Osborne CK and Schiff R (2011) Mechanisms of endocrine resistance in breast cancer. *Annu Rev Med* **62:**233-247.

Paridaens R, Dirix L, Lohrisch C, Beex L, Nooij M, Cameron D, Biganzoli L, Cufer T, Duchateau L, Hamilton A, Lobelle JP, Piccart M, European Organization for the R, and Treatment of Cancer - Investigational Drug Branch for Breast C (2003) Mature results of a randomized phase II multicenter study of exemestane versus tamoxifen as first-line hormone therapy for postmenopausal women with metastatic breast cancer. *Ann Oncol* **14:**1391-1398.

Peterson A, Xia Z, Chen G, and Lazarus P (2017) In vitro metabolism of exemestane by hepatic cytochrome P450s: impact of nonsynonymous polymorphisms on formation of the active metabolite 17beta-dihydroexemestane. *Pharmacol Res Perspect* **5:**e00314.

Petkov PI, Temelkov S, Villeneuve DL, Ankley GT, and Mekenyan OG (2009) Mechanism-based categorization of aromatase inhibitors: a potential discovery and screening tool. *SAR QSAR Environ Res* **20:**657-678.

Platt A, Xia Z, Liu Y, Chen G, and Lazarus P (2016) Impact of nonsynonymous single nucleotide polymorphisms on in-vitro metabolism of exemestane by hepatic cytosolic reductases. *Pharmacogenet Genomics* **26:**370-380.

Plumb RS, Johnson KA, Rainville P, Smith BW, Wilson ID, Castro-Perez JM, and Nicholson JK (2006) UPLC/MS(E); a new approach for generating molecular fragment information for biomarker structure elucidation. *Rapid Commun Mass Spectrom* **20:**1989-1994.

Roth MJ, Dawsey SM, Wang G, Tangrea JA, Zhou B, Ratnasinghe D, Woodson KG, Olivero OA, Poirier MC, Frye BL, Taylor PR, and Weston A (2000) Association between GSTM1*0 and squamous dysplasia of the esophagus in the high risk region of Linxian, China. *Cancer Lett* **156:**73-81.

Santen RJ, Brodie H, Simpson ER, Siiteri PK, and Brodie A (2009) History of aromatase: saga of an important biological mediator and therapeutic target. *Endocr Rev* **30:**343-375.

Schneider F, Boller A, Muller M, Muller P, and Furst A (1973) [The course of the transformation of steroid 3,5-dienamines with formaldehyde]. *Helv Chim Acta* **56:**2396-2404.

Seidegard J, Pero RW, Markowitz MM, Roush G, Miller DG, and Beattie EJ (1990) Isoenzyme(s) of glutathione transferase (class Mu) as a marker for the susceptibility to lung cancer: a follow up study. *Carcinogenesis* **11:**33-36.

Downloaded from dmd.aspetjournals.org at ASPET Journals on April 19, 2024

DMD Fast Forward. Published on September 26, 2018 as DOI: 10.1124/dmd.118.081166
This article has not been copyedited and formatted. The final version may differ from this version.

Shi J, Xie C, Liu H, Krausz KW, Bewley CA, Zhang S, Tang L, Zhou Z, and Gonzalez FJ (2016) Metabolism and Bioactivation of Fluorochloridone, a Novel Selective Herbicide, in Vivo and in Vitro. *Environ Sci Technol* **50:**9652-9660.

Siegel RL, Miller KD, and Jemal A (2017) Cancer statistics, 2017. *CA: A Cancer Journal for Clinicians* **67:**7–30.

Stocco G, Cuzzoni E, De Iudicibus S, Franca R, Favretto D, Malusa N, Londero M, Cont G, Bartoli F, Martelossi S, Ventura A, and Decorti G (2014) Deletion of glutathione-s-transferase m1 reduces azathioprine metabolite concentrations in young patients with inflammatory bowel disease. *J Clin Gastroenterol* **48:**43-51.

Sun D, Chen G, Dellinger RW, Sharma AK, and Lazarus P (2010) Characterization of 17-dihydroexemestane glucuronidation: potential role of the UGT2B17 deletion in exemestane pharmacogenetics. *Pharmacogenet Genomics* **20:**575-585.

van Bladeren PJ (2000) Glutathione conjugation as a bioactivation reaction. *Chem Biol Interact* **129:**61-76.

Wang X and Chen S (2006) Aromatase destabilizer: novel action of exemestane, a food and drug administration-approved aromatase inhibitor. *Cancer Res* **66:**10281-10286.

Zarth AT, Murphy SE, and Hecht SS (2015) Benzene oxide is a substrate for glutathione S-transferases. *Chem Biol Interact* **242:**390-395.

Downloaded from dmd.aspetjournals.org at ASPET Journals on April 19, 2024

DMD Fast Forward. Published on September 26, 2018 as DOI: 10.1124/dmd.118.081166
This article has not been copyedited and formatted. The final version may differ from this version.

Footnotes

Conflicts of interest: There are no competing financial interests or conflicts of interest for any of the authors of this manuscript.

This work was supported by the National Cancer Institute at the National Institutes of Health [Grant R01-CA164366] to P. Lazarus and a China Scholarship Council grant for Shaman Luo.

Downloaded from dmd.aspetjournals.org at ASPET Journals on April 19, 2024

DMD Fast Forward. Published on September 26, 2018 as DOI: 10.1124/dmd.118.081166
This article has not been copyedited and formatted. The final version may differ from this version.

Legends for Figures

Figure 1. UPLC/MS^E analysis of EXE metabolites in urine from a subject taking EXE (Panels A, C, and E) versus chemical standards (Panels B, D, and F). Panels A and B, extracted ion chromatogram of 297.185 (EXE) from channel 1 (intact ion); panels C and D, extracted ion chromatogram of 299.201 (17β-DHE) from channel 1; panels E and F, extracted ion chromatogram of 475.23 (17β-DHE-Gluc) from channel 1.

Figure 2. UPLC/MS^E analysis for Identification of EXE conjugates in urine from a subject taking EXE. Panel A, extracted ion chromatogram of 297.185 from channel 2 (fragment ions in screening for EXE conjugates); panel B, chromatogram of total intact ions of channel 1; panel C, mass spectrum for peak 1 in panel B; panel D, extracted ion chromatogram of 418.206 from channel 1.

Figure 3. UPLC/MS^E analysis for Identification of 17β-DHE conjugates from a subject taking EXE. Panel A, extracted ion chromatogram of 299.201 from channel 2 (fragment ions in screening for 17β-DHE conjugates); panel B, extracted ion chromatogram of 420.22 from channel 1; panel C, mass spectrum for peak 3 in panel B.

Figure 4. UPLC/MS^E analysis of chemically-synthesized and biosynthesized EXE and 17β-DHE cysteine conjugates. Panel A, MS (418.205) chromatography for chemically synthesized 6-EXE-cys standard; Panel B, MS (420.221) chromatography for chemically synthesized 6-17β-DHE-cys standard; Panel C, MS (418.205) chromatography for biosynthesized EXE-cys; Panel D, MS (420.221) chromatography for biosynthesized 17β-

Downloaded from dmd.aspetjournals.org at ASPET Journals on April 19, 2024

DMD Fast Forward. Published on September 26, 2018 as DOI: 10.1124/dmd.118.081166
This article has not been copyedited and formatted. The final version may differ from this version.

DHE-cys; Panel E, MS (421.244) chromatography for biosynthesized D_3-EXE-cys; Panel F, MS (423.240) chromatography for biosynthesized D_3-17β-DHE-cys.

Figure 5. Representative chromatogram for quantification of urinary (Panel A) and plasma (Panel B) EXE and its metabolites in women taking EXE. MS/MS traces for quantification of EXE (297.19>297.19), 17β-DHE (299.20>299.20), 17β-DHE-Glu (475.23>281.19), EXE-cys (418.21>297.19) and 17β-DHE-cys (420.22>299.20) in urine (panel A) and in plasma (panel B) are shown.

Scheme 1. Schematic of EXE metabolism. Shown are major exemestane metabolites formed *in vivo*.

Downloaded from dmd.aspetjournals.org at ASPET Journals on April 19, 2024

DMD Fast Forward. Published on September 26, 2018 as DOI: 10.1124/dmd.118.081166
This article has not been copyedited and formatted. The final version may differ from this version.

Tables

Table 1. MS/MS transitions and ion optic parameters for EXE and EXE metabolites.

	ES+ MS/MS transition (m/z)+	cone voltage (V)	collision energy (eV)
EXE	297.19>297.19	25	10
D_3-EXE	300.20>300.20	25	10
17β-DHE	299.20>299.20	25	10
D_3-17β-DHE	302.22>302.22	25	10
17β-DHE-Gluc	475.23>281.19	20	15
D_3-17β-DHE-Gluc	478.25>284.21	20	15
6-EXE-cys	418.21>297.19	15	15
D_3-6-EXE-cys	421.22>300.20	15	15
6-17β-DHE-cys	420.22>299.20	15	15
D_3-6-17β-DHE-cys	423.24>302.22	15	15

Downloaded from dmd.aspetjournals.org at ASPET Journals on April 19, 2024

Table 2. Summary of EXE metabolite concentrations in plasma and urine from EXE-treated subjects.[a]

	plasma			urine		
	Mean ± SE [b] (nM)	Range	% of TEM [c] (mean ± SE)	Mean ± SE [d] (nmol/mg creatinine)	Range	% of TEM [c] (mean ± SE)
EXE	14 ± 1.7	0-105	17 ± 0.91	0.21 ± 0.045	0-3.2	1.7 ± 0.20
17β-DHE	2.5 ± 0.19	0.11-14	12 ± 1.2	0.0066 ± 0.0012	0-0.099	0.14 ± 0.025
17β-DHE-Gluc	30 ± 4.6	0.32-358	36 ± 1.8	1.4 ± 0.37	0.0068-45	21 ± 1.6
6-EXE-cys	22 ± 2.9	0.020-226	23 ± 1.3	5.9 ± 0.69	0.0033-50	55 ± 1.6
6-17β-DHE-cys	5.9 ± 0.58	0-31	12 ± 0.76	1.8 ± 0.19	0.0033-19	22 ± 0.79

[a] n = 132 subjects taking EXE.
[b] SE = standard error; levels are expressed as nM.
[c] TEM: Total quantified EXE Metabolites = EXE + 17β-DHE + 17β-DHE-Gluc + 6-EXE-cys + 6-DHE-cys. The % of TEM was calculated for EXE or each EXE metabolite for every individual subject, with the mean then calculated for each metabolite of all 132 subjects.
[d] Calculated as nmol/mg creatinine.

Downloaded from dmd.aspetjournals.org at ASPET Journals on April 19, 2024

DMD Fast Forward. Published on September 26, 2018 as DOI: 10.1124/dmd.118.081166
This article has not been copyedited and formatted. The final version may differ from this version.

DMD#81166

Figure 1

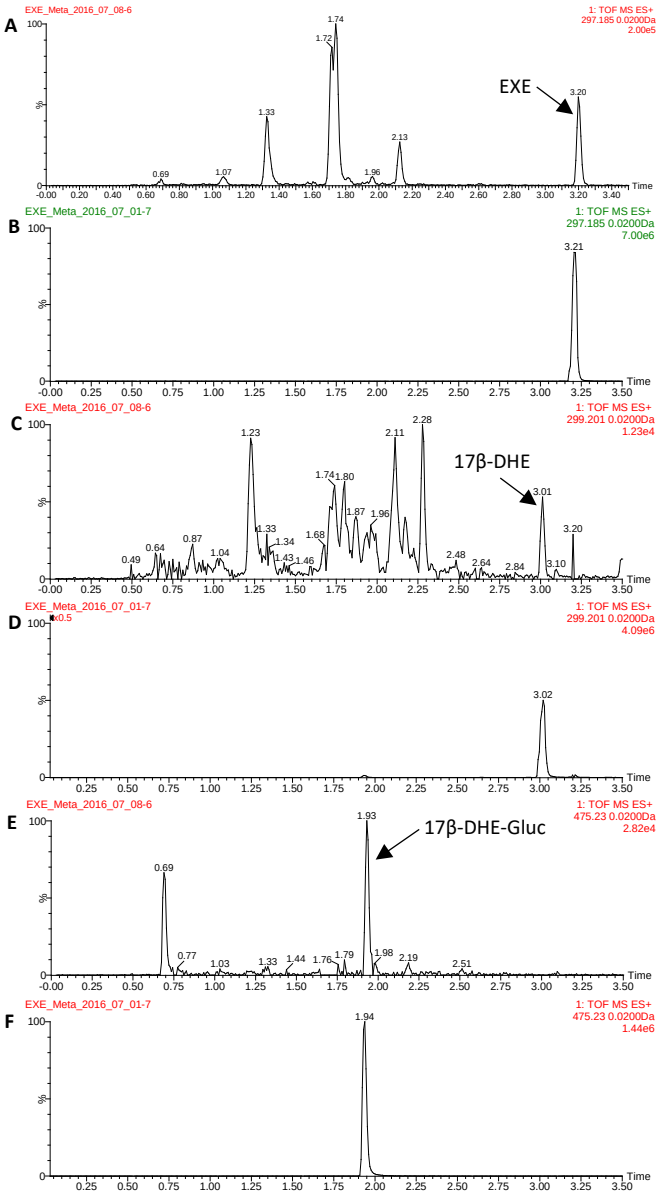

Downloaded from dmd.aspetjournals.org at ASPET Journals on April 19, 2024

DMD Fast Forward. Published on September 26, 2018 as DOI: 10.1124/dmd.118.081166
This article has not been copyedited and formatted. The final version may differ from this version.

DMD#81166

Figure 2

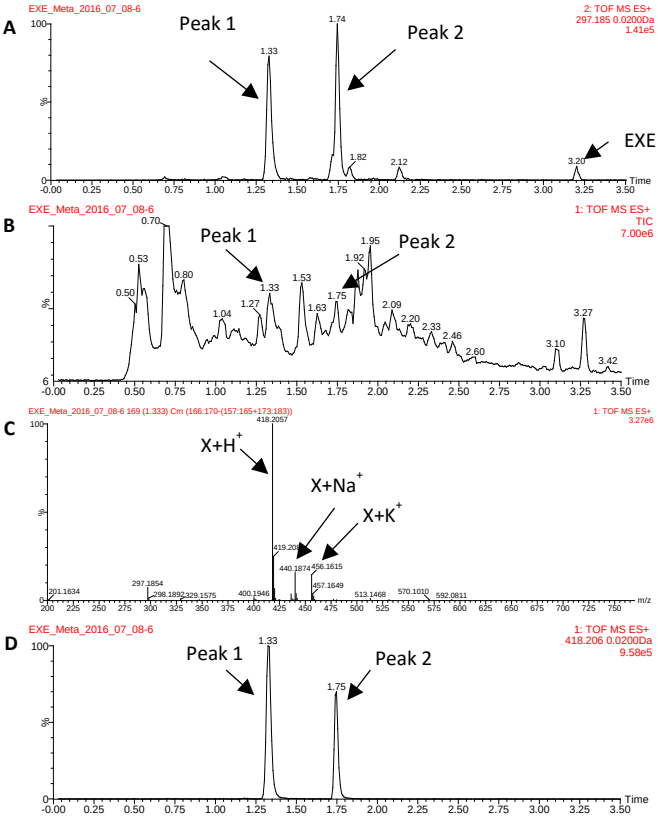

Downloaded from dmd.aspetjournals.org at ASPET Journals on April 19, 2024

DMD Fast Forward. Published on September 26, 2018 as DOI: 10.1124/dmd.118.081166
This article has not been copyedited and formatted. The final version may differ from this version.

Figure 3

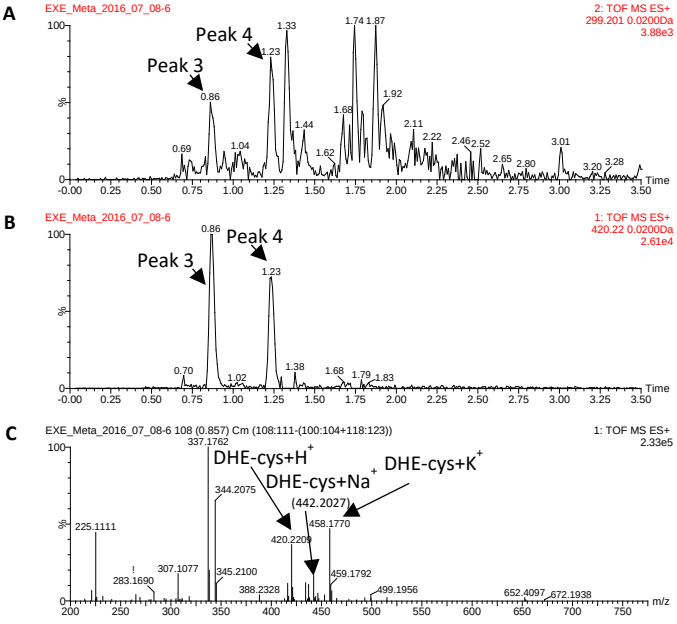

Downloaded from dmd.aspetjournals.org at ASPET Journals on April 19, 2024

DMD Fast Forward. Published on September 26, 2018 as DOI: 10.1124/dmd.118.081166
This article has not been copyedited and formatted. The final version may differ from this version.

Figure 4

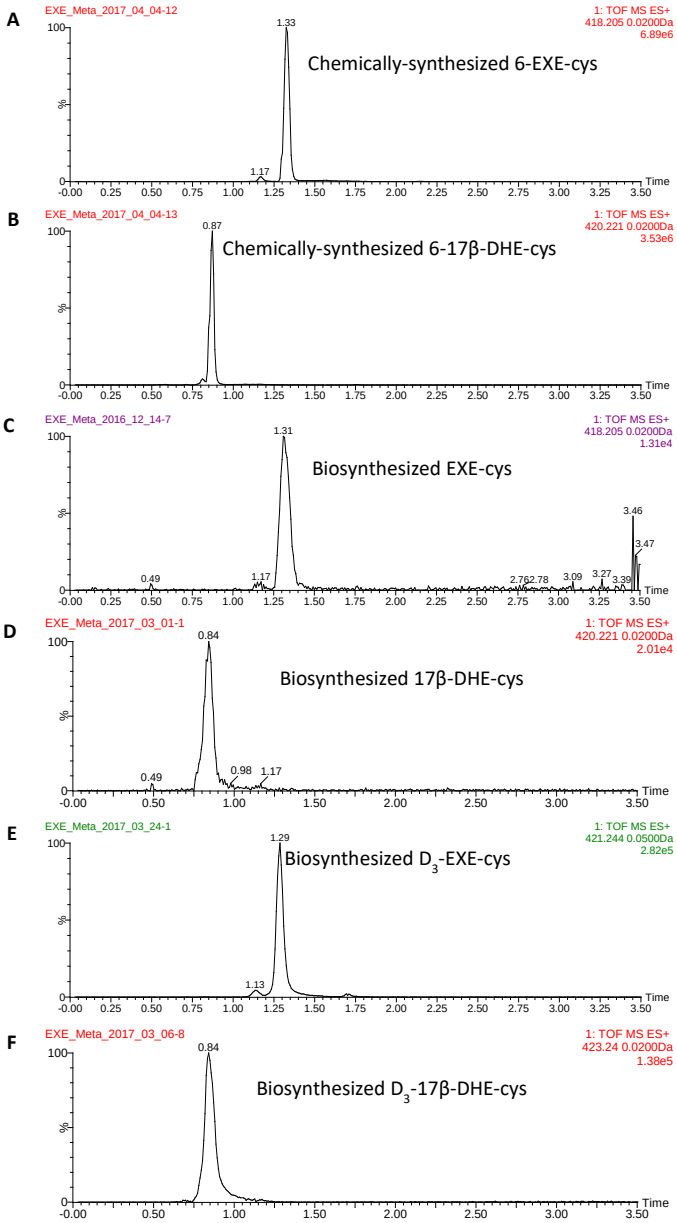

Downloaded from dmd.aspetjournals.org at ASPET Journals on April 19, 2024

DMD Fast Forward. Published on September 26, 2018 as DOI: 10.1124/dmd.118.081166
This article has not been copyedited and formatted. The final version may differ from this version.

DMD#81166

Figure 5

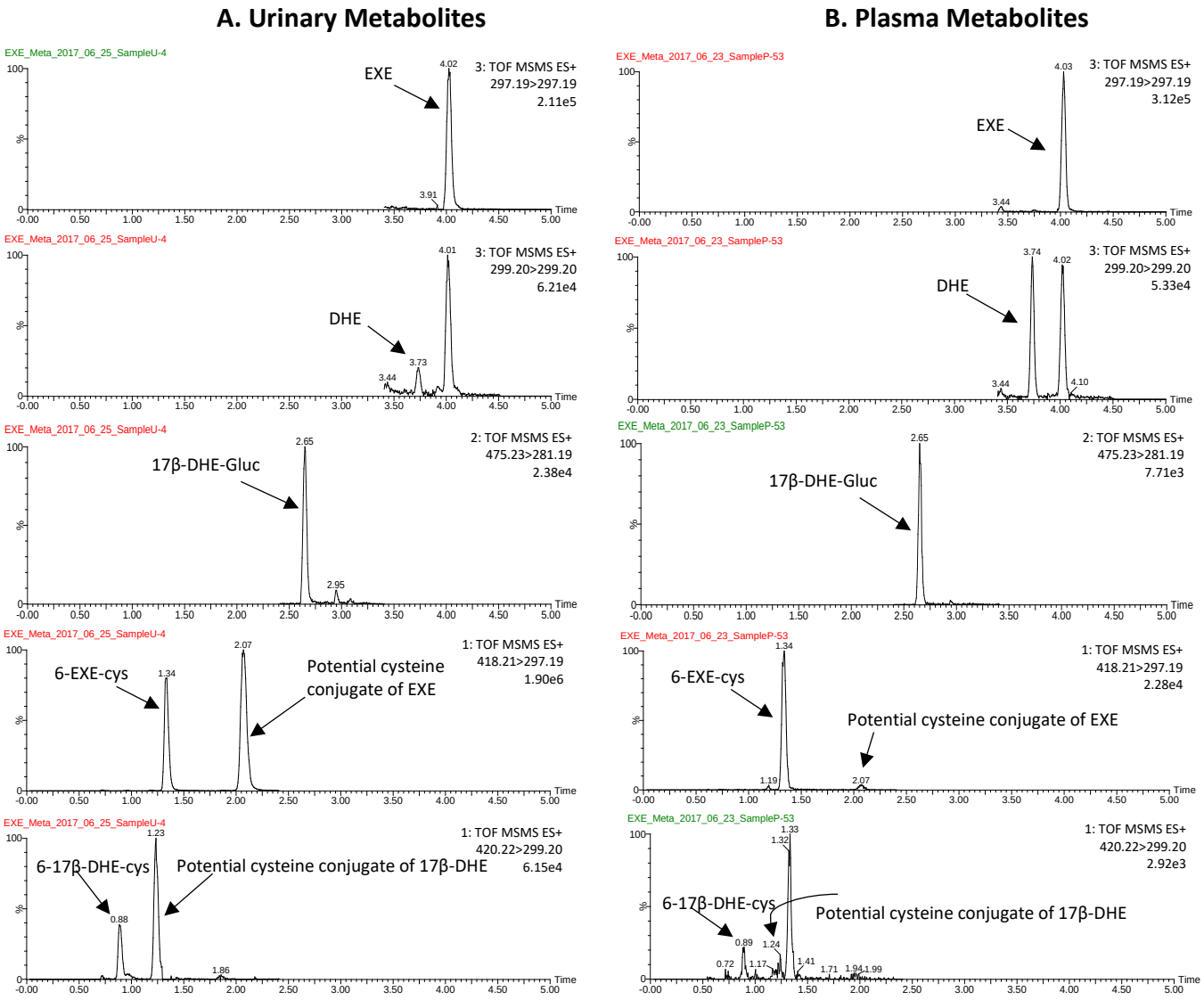

Downloaded from dmd.aspetjournals.org at ASPET Journals on April 19, 2024

DMD Fast Forward. Published on September 26, 2018 as DOI: 10.1124/dmd.118.081166
This article has not been copyedited and formatted. The final version may differ from this version.

Scheme 1

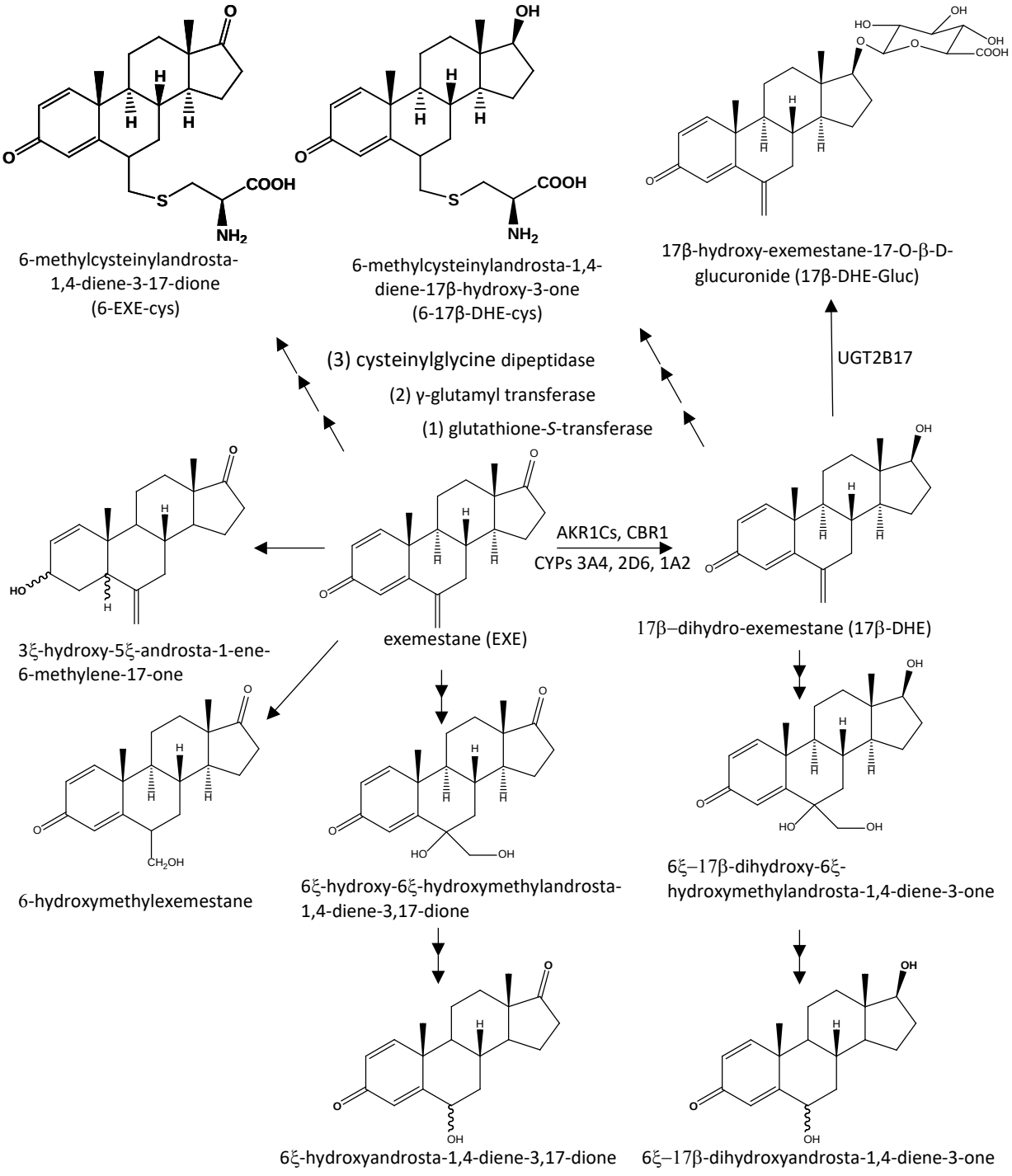

Downloaded from dmd.aspetjournals.org at ASPET Journals on April 19, 2024